

Theoretical modeling of spatial and temperature dependent exciton energy in coupled quantum wells

C. S. Liu,^{1,2} H. G. Luo,^{3,4,5} and W. C. Wu²

¹*Department of Physics, Yanshan University, Qinhuangdao 066004, China*

²*Department of Physics, National Taiwan Normal University, Taipei 11650, Taiwan*

³*Center for Interdisciplinary Studies, Lanzhou University, Lanzhou 730000, China*

⁴*Key Laboratory for Magnetism and Magnetic Materials of the Ministry of Education, Lanzhou University, Lanzhou 730000, China*

⁵*Institute of Theoretical Physics, Chinese Academy of Sciences, Beijing 100080, China*

(Dated: December 26, 2018)

Motivated by a recent experiment of spatial and temperature dependent average exciton energy distribution in coupled quantum wells [S. Yang *et al.*, Phys. Rev. B **75**, 033311 (2007)], we investigate the nature of the interactions in indirect excitons. Based on the uncertainty principle, along with a temperature and energy dependent distribution which includes both population and recombination effects, we show that the interplay between an attractive two-body interaction and a repulsive three-body interaction can lead to a natural and good account for the nonmonotonic temperature dependence of the average exciton energy. Moreover, exciton energy maxima are shown to locate at the brightest regions, in agreement with the recent experiments. Our results provide an alternative way for understanding the underlying physics of the exciton dynamics in coupled quantum wells.

PACS numbers: 71.35.Lk, 71.35.-y, 73.20.Mf, 73.21.Fg.

I. INTRODUCTION

An exciton is a bound pair of an electron and a hole in a semiconductor. At low densities, excitons are Bose quasiparticles with a small mass, somewhat similar to hydrogen atoms. At low temperatures, of the order of 1 Kelvin, the excitons are expected to realize the phenomenon of Bose-Einstein condensation (BEC).¹ Recently, it has been shown that indirect exciton (spatially separated electron-hole pairs) in coupled quantum wells (CQW) can have a long lifetime and high cooling rate. With these merits, Butov *et al.* have successfully cooled the trapped excitons to the order of 1 K.² Although there is not enough evidence to prove that these excitons are condensed into the BEC state, it is fascinating enough to observe several novel features of the photoluminescence (PL) patterns.^{3,4}

Major features of the macroscopically ordered exciton states observed are summarized as follows.^{3,4} (i) Two exciton rings are formed. When the focused laser is used to excite the sample and prompt luminescence is measured in the vicinity of the laser spot, a ring, called the internal ring, is formed. A second ring of PL appears away from the source at the distance about 1 mm, called the external ring. (ii) The intervening region between the internal and external rings are almost dark except for some localized bright spots. (iii) Periodic bright spots appear in the external ring. The bright spots follow the external ring either when the excitation spot is moved over the sample, or when the ring radius is varied with the excited power. (iv) PL is washed out eventually with increasing temperatures. (v) In an impurity potential well, the PL pattern becomes much more compact than a Gaussian with a central intensity dip, exhibiting an annular shape

with a darker central region. (vi) With the increase of the laser power, exciton cloud first contracts then expands. (vii) Exciting sample by higher-energy lasers, the dip can turn into a tip at the center of the annular cloud.

The above experimental facts raised several interesting questions which need to be clarified. (i) What is the reason behind the two-ring structure? (ii) What is the physical origin of the periodic periodic bright spots in the external ring? And, (iii) is this a coherent phenomenon, or a result due to unbalanced transportation? In Ref. 5, a charge separated transportation mechanism was proposed. It gave a satisfactory explanation to the formation of the exciton ring and the dark region between the internal and external rings. However, the remaining two questions are still not clarified satisfactorily.

It is commonly believed that the periodic bright spots in the external ring are formed due to certain kind of instability. It generates the density modulation by a positive feedback. Regarding the origin of the instability, Levite *et al.* considered that exciton states are highly degenerate and the instability comes from the stimulated scattering.⁶ When a local fluctuation occurs in the exciton density, it will lead to an increase in the stimulated electron-hole binding rate. The depletion of local carrier concentration then causes neighboring carriers to stream towards the point of fluctuation. On the other hand, Sugakov suggests that the instability is due to an attractive interaction between the high-density excitons.⁷ The creation of different structures, for example, the islands or the rings of the condensed phase, occurs due to the nonequilibrium state of the system connected with the finite value of the exciton lifetime and the presence of pumping. Therefore, the appearance of the patterns is likely a consequence of self-organization processes in a

nonequilibrium system.⁸

To understand the subtle properties of indirect exciton, further experiments have been done and reported. For example, a novel method was proposed to demonstrate that cold exciton gases can be trapped by the laser induced trapping, which is similar to the trapping of BEC ultracold atoms.⁹ More recently, an improved trapping technique was used to lower the effective temperature of indirect excitons.¹⁰ With the even low temperature, four narrow PL lines have been observed, which corresponds to the emission of individual states of indirect excitons in a disorder potential. The homogeneous line broadening increases with density and dominates the linewidth at high densities.

In a recent paper (Ref. 11), for the first time, Yang *et al.* measured the exciton PL energy along the circumference of the ring. The most interesting result is that the average exciton energy depends on temperature *nonmonotonically*. With reducing temperatures, average exciton energy of the indirect exciton is lowered until the transition temperature, $T_{tr} \simeq 4$ K, is met. Below T_{tr} , the macroscopically ordered exciton state is formed but the average exciton energy in the ring actually increases with temperature being further lowered. In particular, the largest energy of single exciton is found to locate in the brightest regions. Due to these observations, Yang *et al.*¹¹ argued that the interaction between exciton is repulsive. A numerical calculation seems to support this scenario.¹²

Another important experiment is the measurement of the coherence length. A Mach-Zehnder interferometer with spatial and spectral resolution was used to probe the spontaneous coherence in cold exciton gases, which are implemented experimentally in the ring of indirect exciton in CQW.¹³ A strong enhancement of the exciton coherence length is observed at temperatures below a few Kelvin. The increase of the coherence length is correlated with the macroscopic spatial ordering of excitons. The coherence length at the lowest temperature corresponds to a very narrow spread of the exciton momentum distribution, much smaller than that of a classical exciton gas. It also shows that the apparent coherence length is well approximated by the quadratic sum of the actual exciton coherence length and the diffraction correction given by the conventional Abbe limit divided by π .¹⁴

Whether the interaction between excitons in the macroscopically ordered state is attractive or repulsive and to what extent the interaction affects the formation of the macroscopically ordered state remain an open question. The current paper attempts to clarify the above issues. In fact, experimental data had revealed several important clues. After analyzing the experimental facts, it is found that attractive interaction is dominant in indirect excitons and their nonequilibrium distribution plays an important role in the macroscopically ordered state. Moreover, the uncertainty principle is shown to lead to a good account for the experimental phenomena and numerical simulations have confirmed that.

This paper is organized as follows. In Sec. II, based on the uncertainty principle, we present a qualitative analysis of the temperature dependence of the average exciton energy in the external exciton ring. No interaction is considered in this section. In Sec. III, the uncertainty principle is used again to explain the particle number density dependence of the PL FWHM (full width at half maximum) broadening and energy shift. The PL spectra, which are broadened first and then become sharper, provide a strong evidence of the competition between a two-body attraction and a three-body repulsion. In Sec. IV, we use a phenomenological nonlinear Schrödinger equation, together with a temperature and energy dependent exciton distribution, to discuss the exciton energy spatial distribution in the external ring. The largest energy of single exciton is found to be in the brightest regions. In Sec. V, temperature dependence of the average exciton energy in the external ring is studied quantitatively using the approach proposed in Sec. IV. The calculation shows that average exciton energy first decreases and then increases with increasing temperatures. In Sec. VI, we give a demonstration on the exciton distribution in the laser induced trap case. Sec. VII is devoted to a brief summary.

II. TEMPERATURE DEPENDENCE OF ENERGY: QUALITATIVE ANALYSIS

To understand the experimental phenomena, we first analyze the electron and hole creation, transportation, and the exciton formation qualitatively. As pointed out in Refs. [5,15], when electrons and holes are excited by lasers, they are hot electrons and hot holes initially. Since the drift speed of hot electrons is larger than that of hot holes (electron has a smaller effective mass), electrons and holes are indeed charge-separated at this stage (no true exciton is formed). Because hot electrons and holes have a small recombination rate and optical inactive, they can travel a very long distance from the laser spot. After a long-distance travel, hot electrons and holes collide with the lattices and are eventually cooled down. Due to the neutrality of the CQW, negative charges will slow down and accumulate far away from the laser spot. As a consequence, spatially separated electrons and holes form excitons and become optical active at the boundary of the opposite charges where they recombine and show a sharp luminescence ring. This kind of charge separated transportation mechanism has been used to interpret the exciton ring formation.^{5,15}

It should be emphasized that, however, after the long-distance transportation and cooling, cooled electrons and holes will meet in the region of the external ring in the experiment of Butov *et al.*³ However, in the experiment of Lai *et al.*⁴, they meet in the impurity potential well. It is believed that only cooled electrons and holes can form excitons. At this stage, charges are not separated, but coupled or bound together. The long lifetime of the ex-

citons means the lower electron-hole recombination rate. Therefore the elemental particles in the external ring³ and in the impurity potential well⁴ are *excitons*. We thus argue that it is the interaction between excitons, rather than the unbalanced transportation, which leads to the nonhomogeneous density distribution associated with the complex PL patterns.

When the experimental temperature is low ($T \lesssim 1.4$ K), average translational kinetic energy and in-plane momentum of excitons are also low. In such case, excitons are optically active and the space-dependent PL intensity is proportional to the exciton number distribution. Since exciton number distribution is equal to the product of the probability distribution and the total exciton number N , if N remains unchanged, PL intensity is directly proportional to the probability distribution. In the following discussion, we simply take exciton density distribution as the PL distribution. Besides, since particles can only move within the CQW, their motions are essentially two-dimensional (2D).

The periodic array of beads in the external rings is a low-temperature phenomenon. This means that average exciton translational kinetic energy is low enough and its wave-particle duality is important. Therefore exciton energy is governed by the uncertainty principle. The uncertainty principle predicts that $\Delta p \sim \hbar/\Delta r$, where Δp is the momentum spread, Δr is spatial uncertainty, and \hbar is the Planck's constant. Since exciton's momentum can be approximated by $p \sim \Delta p$, the corresponding energy $E \sim \hbar^2/[2m(\Delta r)^2]$. With these in mind, one is able to consider the temperature dependence of the exciton energy distribution, such as those reported in Ref. 11. When temperature is lower than $T_{tr} \simeq 4$ K, macroscopic ordered state forms. Exciton are confined into each bead of the external ring. Their spatial uncertainty Δr can be approximated by the diameter R of the bead ($\Delta r \simeq R$). Experiments have observed that the lower the temperature is, the higher contrast the pattern is and the smaller the R is.¹¹ This implies that when temperature is lower, momentum uncertainty will be larger and hence the exciton energy will be higher. This gives a qualitative interpretation why the average exciton energy increases with decreasing temperatures.

When temperature is increased to be higher than T_{tr} , macroscopically ordered state breaks down and the confined regions enlarge essentially. The uncertainty related energy will decrease in principle. However, when the temperature is increased further, the system undergoes a transition into the classical limit to which wave character of exciton is no longer important. In this case, the average exciton translational kinetic energy is directly proportional to the temperature. Therefore, non-monotonic temperature dependence of the average exciton energy is closely related to the pattern formation, and has little to do with the interaction between excitons. In Fig. 3 of Ref. 11, linear temperature dependence of the average exciton energy is reported at $T > T_{tr}$. Their results confirmed that excitons behave classically in this limit

to which $E \sim k_B T$ at 2D. Nevertheless, the slope of the linear temperature dependence was measured in Ref. 11 to be about 1.4×10^{-4} eV K^{-1} , slightly larger than the Boltzman constant, $k_B = 8.62 \times 10^{-5}$ eV K^{-1} . The difference may be due to some effect of the interactions and extra degrees of freedom in addition to translational motions.

III. EXCITON PL SPECTRA: QUALITATIVE ANALYSIS

For a long time, indirect exciton PL FWHM energy and the shift with increasing density in the presence of a random potential remain to be fully understood.^{10,16} In a previous paper¹⁷, we have proposed a mechanism to study the macroscopically ordered exciton states. The most important point lies in the interaction which involves the competition between a two-body attraction and a three-body repulsion. Here we elaborate this point, along with the uncertainty principle, to illustrate the PL spectra.

It is instructive to emphasize several important features in connection with our model. The idea first came from the density dependence of inhomogeneous exciton distribution. It is clear that the interaction between the indirect exciton is neither purely attractive, nor purely repulsive. If the interaction between the indirect exciton is purely repulsive, it will drive the exciton towards homogeneous distribution and the exciton cloud will expand with the increase of the exciton number. On the contrary, if the interaction is purely attractive, the system is expected to collapse when the exciton density is greater than a critical value to which there is not enough kinetic energy to stabilize the exciton cloud. In addition, the case of a purely repulsive or a purely attractive interaction is incapable to understand the experimental fact that the exciton cloud contracts first and expands later when the laser power is increased.⁴

The existence of the attractive interaction does not mean that the exciton state is unstable against the formation of metallic electron-hole droplet. The reason is that the repulsive interaction may dominate over the attraction in that regime and keep the system stable. Many effects may contribute to the exciton interaction. The most important one is the exciton dipole-dipole interaction. Exciton behaves like a dipole, so a strong repulsion will govern exciton interaction when two dipoles are aligned parallel. However, if the direction of two dipoles changes from aligned parallel to inclined, the attraction between the election of one exciton and the hole of the other exciton will dominate. This case can happen easily when exciton density is low. In case of high densities, due to the strong Coulomb interaction, the dipoles will tend to align parallel and consequently a repulsive interaction dominates. The other important interaction originates from the exchange effect. When two indirect exciton approach to each other, the exchange interaction

between two electrons, as well as the one between two holes become important. This may be another source of the attractive interaction between excitons.

In fact, the complex exciton interaction which results from the competition of multi-effects, may be well described by the van der Waals form. It has pointed out that the effective interaction between exciton will be attractive when the separation between two exciton is about 3 to 6 exciton radii.⁷ In the current experiment, the exciton density is about $10^{10}/\text{cm}^2$. For this density, the average distance between the indirect exciton is about 100 nm. As the exciton Bohr radius a_B is about $10 \sim 50 \text{ nm}^4$, the average distance between excitons is about $2 \sim 10$ exciton radii. Thus it is reasonable to assume that the two-body interaction is in the attractive regime. In fact, the attractive interaction between the exciton has been considered as a possible candidate to describe the pattern formation observed by experiments.^{7,18}

In a previous paper¹⁷, taking into account the two-body attraction and the three-body repulsion interactions, we have proposed that in the dilute limit the behavior of the exciton can be described by a *nonlinear* Schrödinger equation¹⁷

$$-\frac{\hbar^2}{2m^*}\nabla^2\psi_j + (V_{ex} - g_1n + g_2n^2)\psi_j = E_j\psi_j, \quad (1)$$

where ψ_j and E_j are the j -th eigenstate and eigenvalue, respectively. V_{ex} is an external potential, and g_1 and g_2 are (positive) coupling constants associated with two-body and three-body interactions. $n = n(\mathbf{r})$ is the local density of exciton and at the mean field level,

$$n(\mathbf{r}) = \sum_{j=1}^{\mathcal{N}} \eta_j(E_j) |\psi_j(\mathbf{r})|^2, \quad (2)$$

where \mathcal{N} denotes the total number of bound states and η_j is the corresponding probability function associated with the energy level E_j . η_j satisfies the normalized condition $\sum_{j=1}^{\mathcal{N}} \eta_j(E_j) = 1$. Readers can refer to Ref. 17 for a detailed description of the model.

In the present model, when macroscopically ordered state forms in the ring or in the impurity (disorder) potential well, exciton will distribute over the discrete energy levels. In fact, four sharp peaks in PL spectra corresponding to the emissions of indirect exciton states have been observed recently in a so-called "elevated trap".¹⁰ We attribute the individual localized states as the confinement due to both the elevated trap potential and the self-trapped potential (arising from the attractive interaction).

The present model can give a natural and self-consistent explanation of the particle density dependence of FWHM broadening and PL energy shift. For low density exciton, the interaction between exciton is dominated by the attraction. With the increase of the particle density (by increasing the laser power), the low temperature exciton cloud will contract irrespective of localized or delocalized states. This means that the attractive interaction hampers the exciton motion. At the mean field level,

this corresponds to the increase of the self-trapped potential. The larger the particle density is, the larger the attractive interaction is, and the exciton cloud will contract further. At low temperature, $T < T_{tr}$, uncertainty principle governs the exciton motion. Consequently, it results in higher mean exciton energy and larger energy dispersion. Higher mean exciton energy indicates blue-shift of PL peak and larger energy dispersion means that PL peak is more broadened (FWHM becomes large).

When the particle density is further increased, three-body repulsion becomes more important and self-trapped interaction becomes weaker. The PL peaks will red shift and become sharp again. In fact, with the increase of the laser power in the low particle density regime, the phenomenon that PL spectra broaden first and then become sharper has been observed (see Fig. 3(c) of Ref. 10). This, in addition to the support given by the experimental data in Ref. 4, provides a further evidence that the interaction between exciton is likely the combination of a two-body attraction and a three-body repulsion. With increasing the laser power, blue shift of the PL peaks has been reported in Ref. 19. However, the prediction of blue shift first and then red shift of the PL peak with the increase of the laser power has not been observed yet! Further experiments are in demand.

IV. SPATIAL ENERGY DISTRIBUTION

In order to study the spatial dependence of the energy distribution in the external exciton ring, it is necessary to solve the nonlinear Schrödinger equation (1) numerically. In addition to the assumption of interactions, another important aspect lying in our model is the disequilibrium energy disequilibrium energy distributions of indirect excitons. In fact, the indirect excitons in CQW involves both the (complex) energy relaxation and recombination processes. These have been studied by several experimental and theoretical groups.²⁰ It shows that for a relaxation process, when the exciton density is low ($n \ll a_B^2$, a_B is Bohr radius), the effects due to the exciton-exciton interaction and the exciton-carrier scattering can be neglected. In this case, the relaxation time is mainly determined by the scattering of excitons with acoustic phonons.²¹ In particular, at low bath temperatures ($T_b < 1 \text{ K}$), this kind of relaxation rate decreases dramatically due to the so-called "phonon bottleneck" effects.²⁰

For the recombination process, on the other hand, because exciton in the lowest self-trapped level are quantum degenerate, they are dominated by the stimulated scattering when the occupation number is more than a critical value. Strong enhancement of the exciton scattering rate has been observed in the resonantly excited time-resolved PL experiment²². Therefore, even though the phonon scattering rate is still larger than the radiative recombination rate, thermal equilibrium of the system may not be reached. Essentially the distribution $\eta_j(E_j)$

may deviate significantly from the usual Boltzmann or Bose like.²³

A recent paper (Ref. 10) reported that the observed narrow PL lines of indirect excitons in a disorder potential correspond to the emission of individual states. It has been shown that the intensity of PL spectra is roughly in proportion to the exciton number. When excitons distribute over some given energy levels, the PL spectra will exhibit strong peaks corresponding to these levels. Therefore the relative height of the PL peaks can be interpreted as the exciton distribution probability associated with the energy level, $\eta_j(E_j)$.

At the high temperature of 10 K, the PL peak intensity of the high excited state is higher than that of the ground state (see Fig. 2(c) of Ref. 10). This indicates that exciton have a larger probability distribution in the high excited state. With reducing the temperature to 5.1 K, the PL peak intensity becomes lower for the high excited state while it becomes higher for the other three peaks associated with the two ground states. It seems that excitons at higher states will relax to lower states when the temperature is reduced. At the temperature lower than 5.1 K, the intensities are found to be almost identical for the four peaks. It indicates that excitons distribute over the four discrete levels with almost the same probability. Furthermore, at even lower temperature of 2.7 K, the low-energy peaks become very dim. This implies that phonon bottleneck effect is in effect for ground state and low excited states and in this regime, excitons in high excited states are having difficulty relaxing to the ground states.

From the above analysis, one can generalize $\eta(E_j) \rightarrow \eta(E_j, T)$ to have a better description for the temperature dependence of particle number distribution of bound states. As mentioned above, experiment seems suggesting that the weight of $\eta(E_j, T)$ will transfer from high-energy states to low-energy states when T is decreased. It also suggests that, for a given T , the weight of $\eta(E_j, T)$ is larger in higher-energy states than that in lower-energy states. With the above in mind, two other factors are also important in determining the actual form of $\eta(E_j, T)$. Firstly, exciton are Bose quasiparticle and at not too low temperatures, the distribution can be approximated by the (classical) Boltzmann function, $\exp(-E_j/T)$, where T is considered as an effective temperature related to lattice temperature. The other important factor is the energy dependence of exciton luminescence efficiency. Low-energy excitons is more optical active than that of high energy exciton. So the low energy excitons have a high luminescence efficiency which is contrary to the high-energy excitons. Thus low-energy state will have relatively smaller exciton distribution taking into account the luminescence efficiency. One can use $\exp(E_j/E_0)$ to describe qualitatively this effect, where E_0 is an effective energy scale related to the exciton life time. As a consequence, temperature and energy dependent exciton distribution is an outcome of the competition between the above two effects. We then take the following *phenomenological* form

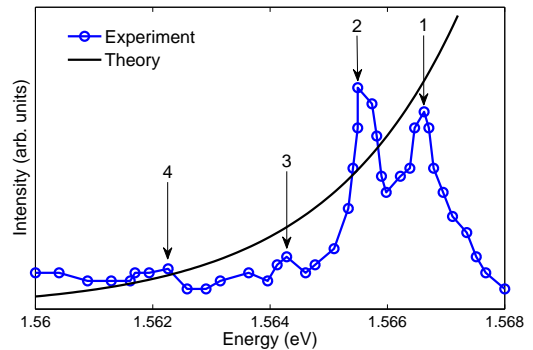


FIG. 1: Energy dependent exciton distribution. Solid line is obtained from the phenomenological formula (3) with chemical potential $\mu = 1.56$ eV and $\alpha = 0.025$ eV⁻¹. Circle line corresponds to the exciton PL spectra (in arbitrary unit) taken from Fig. 2(a) of [10]. For comparison, a constant is multiplied to the solid line.

for the weight

$$\begin{aligned} \eta(E_j, T) &\equiv C \exp[-(E_j - \mu)/T] \exp[(E_j - \mu)/E_0] \\ &= C \exp[\alpha(E_j - \mu)], \end{aligned} \quad (3)$$

where C is the normalization factor, μ is the chemical potential, and $\alpha \equiv 1/E_0 - 1/T$. Typically $E_0 < T$ and hence $\alpha > 0$. When temperature and laser power remain unchanged, μ and α will remain constantly. While increasing the temperature, α will increase correspondingly. Thus α can be considered as an "effective temperature".

Equation (3) basically gives an appropriate temperature and energy dependent probability density distribution for indirect exciton. In Fig. 1, we compare the theoretical curve [based on Eq. (3)] with the experimental PL spectra reported in Ref. 10. The experimental data (circles) in Fig. 1 are in arbitrary unit. For comparison, we have multiplied a constant to the probability density. It should be mentioned that we have tried various distribution functions and found that Eq. (3) gives the best fitting. In our earlier study (Ref. 17), we have assumed that exciton are distributed at different energy levels with almost the same probability. Strictly speaking, it corresponds only to the low temperature limit in Eq. (3).

Numerically it is convenient to do the following scaling: $\psi_j(\mathbf{r})/\sqrt{N} \rightarrow \psi_j(\mathbf{r})$, $Ng_1 \rightarrow g_1$, and $N^2g_2 \rightarrow g_2$, such that Eq. (1) remains the same form. In this case, $n(\mathbf{r})$ becomes the probability density which satisfies the normalization condition $\int_S n(\mathbf{r})dS = 1$. After further rescaling $\psi_j(\mathbf{r})\sigma_{\text{PL}} \rightarrow \psi_j(\mathbf{r})$ and $\mathbf{r}/\sigma_{\text{PL}} \rightarrow \mathbf{r}$, Eq. (1) is reduced to

$$-\frac{1}{2}\nabla^2\psi_j + (v_{ex} - a_1n + a_2n^2)\psi_j = \varepsilon_j\psi_j, \quad (4)$$

where $v_{ex} \equiv V_{ex}/\epsilon$, $a_1 \equiv g_1/(\sigma_{\text{PL}}^2\epsilon)$, $a_2 \equiv g_2/(\sigma_{\text{PL}}^4\epsilon)$, and $\varepsilon_j \equiv E_j/\epsilon$. Here $\epsilon \equiv \hbar^2/m^*\sigma_{\text{PL}}^2$ with σ_{PL} being the

root-mean-square radius of the exciton cloud observed by photoluminescence. With the above scaling, it is found that $a_1^2/a_2 = g_1^2/g_2\epsilon = g_1^2 m^* \sigma_{\text{PL}}^2 / g_2 \hbar^2$, which is a constant for an explicit sample.

Taking into account the experimental facts,^{3,11} two important points should be clarified. (i) The exciton patterns are fully determined by its self-trapped interactions. External potential V_{ex} is not the main cause for complex exciton patterns. Thus we set $v_{ex} = 0$ for simplicity. (ii) When an electron and a hole form an exciton at low temperature, it is believed that their kinetic energy is low and all exciton are and all exciton are self-trapped. Particles with energy greater potential energy can not be bounded in the self-trapped well and should be ruled out in the calculations.

The mean kinetic energy of excitons can be given by

$$E_k = \int \int dxdy E_k(x, y), \quad (5)$$

where $E_k(x, y)$ is the mean local (space-dependent) kinetic energy density. Considering the probability function of each level, $\eta_j \equiv \eta(E_j, T)$, E_k can also be given by

$$E_k = \sum_{j=1}^{\mathcal{N}} \eta_j E_{kj}, \quad (6)$$

where E_{kj} is the kinetic energy associated with level j . In fact,

$$\begin{aligned} E_{kj} &= - \int \int dxdy \psi_j^*(x, y) \nabla^2 \psi_j(x, y) \\ &= \int \int dxdy \left(\left| \frac{\partial \psi_j(x, y)}{\partial x} \right|^2 + \left| \frac{\partial \psi_j(x, y)}{\partial y} \right|^2 \right), \end{aligned} \quad (7)$$

with $\psi_j(x, y)$ the wave function of level j . In obtaining the 2nd line of Eq. (7), an integration by parts and a boundary condition that wave function vanishes at the infinity (bound states) are applied. By comparing Eqs. (5)–(7), the mean spatial energy density is obtained to be

$$E_k(x, y) = \sum_{j=1}^{\mathcal{N}} \eta_j \left(\left| \frac{\partial \psi_j(x, y)}{\partial x} \right|^2 + \left| \frac{\partial \psi_j(x, y)}{\partial y} \right|^2 \right). \quad (8)$$

Besides, one can also obtain the angle dependent kinetic energy density via

$$E_k(\theta) = \int_{(x, y) \in (\theta, \theta + \Delta\theta)} dxdy E_k(x, y) \quad (9)$$

with $\tan \theta \equiv y/x$. In Fig. 2(a), we show both the particle density distribution, $n(\mathbf{r})$, in the exciton ring and the angle-dependent kinetic energy distribution, $E_k(\theta)$. Obviously the maxima of $E_k(\theta)$ are located at the center of the beads. Fig. 2(b) shows the spatial dependence of the kinetic energy distribution, $E_k(x, y)$. One interesting feature is that $E_k(x, y)$ is zero at the center of the beads. This can be elucidated by future experiments of finer resolution.

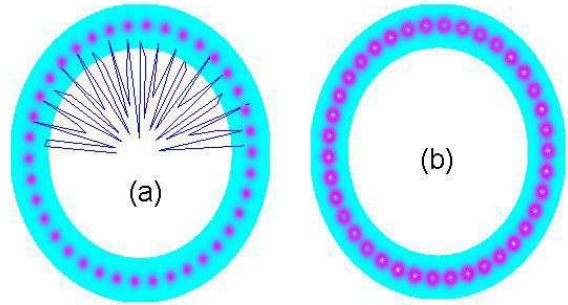


FIG. 2: (a) Formation of the macroscopically ordered state of the exciton ring at very low temperatures. The corresponding angle-dependent energy distribution $E_k(\theta)$ (solid line) is also shown. (b) Spatial distribution of the kinetic energy, $E_k(x, y)$. Parameters used are $a_1 = 250$, $a_2 = 0.001a_1^2$, effective temperature $\alpha = 0.002$, and chemical potential $\mu = 0$.

V. TEMPERATURE DEPENDENCE OF ENERGY: QUANTITATIVE RESULTS

In section II, with the uncertainty principle, a qualitative analysis was made on the temperature dependence of exciton average energy in the external ring. Here we solve the nonlinear Schrödinger equation (1), together with the disequilibrium distribution $\eta_j(E_j, T)$, to study the temperature dependence quantitatively. As mentioned before, α can be treated as an effective temperature in the present case. Temperature (α)-dependent exciton ring patterns are shown in Fig. 3(a)-(c), while Fig. 3(d) shows the nonmonotonic temperature dependence of the total energy, $E_k = \int E_k(\theta) d\theta$.

It should be noted that our theory applies only to low temperatures when excitons are in or near the condensed state. When temperature is above the critical point, such as $T_{tr} \simeq 4$ K presented in Ref. 10, excitons will transfer from condensed to non-condensed phase. Above T_{tr} in the non-condensed phase, the exciton liquid may be “boiling” and its spatial distribution could change with the time. At such high temperatures, our theory will break down to which numerical calculation turns no convergent solutions. In fact, the exciton pattern shown in Fig. 3(c) is just a snapshot of time-dependent exciton number distribution. When $\alpha \gtrsim 0.08$ in our numerical simulation, the exciton behavior can be well described by the classical statistical physics and a linear formula $\epsilon = k_B T$ is plotted in Fig. 3(d) for illustration purpose.

A brief summary is in order here. Initially, if exciton are uniformly distributed on the external ring, attractive interaction will drive the exciton to approach each others. When the local density reaches a critical value, the kinetic energies of the exciton will drive the high-density excitons to diffuse. At the same time, the repulsive in-

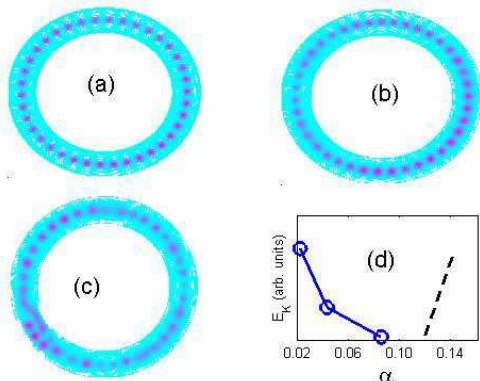


FIG. 3: Formation of the macroscopically ordered state of the exciton ring at different effective temperatures: (a) $\alpha = 0.002$, (b) $\alpha = 0.004$, and (c) $\alpha = 0.008$. (d) Temperature (α) dependence of the total energy E_k . All other parameters are taken to be the same as those in Fig. 2.

teraction, which increases with the density, will hinder further increase of the exciton density. As a result, an array of clusters on the external ring forms. The size of these clusters is thus determined by three factors, i.e., the attractive interaction, the three-body repulsive interactions, and the kinetic energies of the excitons associated with the temperatures. This is the basic idea behind our model on the macroscopically ordered states of excitons.

Finally some remarks on the temperature effect are given. When the bath temperature is low, cooled excitons have relatively low momenta and the self-trapped interaction is able to confine most of the excitons. However, in the low momentum case, cooling efficiency is low while luminous efficiency is high, excitons can not reach the thermal equilibrium state. At the meantime, due to the competition between the self-trapped and the kinetic energies, complex exciton patterns occur (as discussed above). With increasing the temperature, the exciton can not be fully cooled and correspondingly self-trapped interaction confines only part of the excitons. The attractive interaction also cannot compensate the exciton kinetic energy and excitons will distribute homogeneously in a 2D plane. In this case, the pattern is washed out. If the temperature is higher than the indirect exciton binding energy ~ 3.5 meV,^{24,25} most of excitons become ionized and are in a plasma state. No pattern can be observed in this case.

VI. NUMBER DISTRIBUTION WITH LASER INDUCED TRAP

Similar to the studies of ultracold alkali atoms and molecules, the laser-induced trapping was proposed and demonstrated for a highly degenerate Bose gas of exciton.⁹ An important advantage of laser trapping is

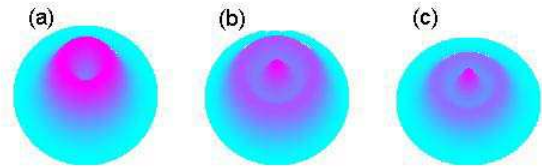


FIG. 4: The exciton distribution in laser-induced trap for (a) low ($a_1 = 15$), (b) intermediate ($a_1 = 23$), and (c) high ($a_1 = 35$) densities. The other parameters are taken to be same as those in Fig. 2.

that it is possible to control the trap in situ by varying the laser intensity in space and time. A commonly seen phenomenon for highly degenerate excitons is its annular particle distribution in the laser-induced trap. We argue that this kind of distribution is similar to that found in an impurity potential reported in Ref. 4. In our previous work, a detailed discussion was already given to this kind of trapped exciton distribution.¹⁷ Since laser induced trapping can confine higher density exciton, it is hoped that the experiment can also be done at very high densities to explore the many-body physics of excitons.

Using the temperature and energy dependent distribution given in Eq. (3) together with a two-dimensional pseudopotential

$$v_{ex}(\mathbf{r}) = \begin{cases} -5 & \text{for } r \leq \sigma_{PL} \\ 0 & \text{otherwise,} \end{cases} \quad (10)$$

we solve the nonlinear Schrödinger equation (1) for exciton number distribution ranging from low to high densities. The results are presented in Fig. 4. As mentioned before, σ_{PL} is the root-mean-square radius of the exciton PL pattern. To compare to experiments, we take $a_1 = 15, 23, \text{ and } 35$ with $a_2 = 0.004a_1^2$ accordingly. As shown in Fig. 4, the excitons distribute annularly at low densities and at high densities, some fine structures develop at the center of the ring, which is consistent with the experiments. Readers can refer to Ref. 17 for the reason behind the annular distribution and some related physics.

VII. SUMMARY

In summary, the uncertainty principle is used to analyze the spatial and temperature dependence of the average exciton energy distribution in a macroscopically ordered state of the exciton. The competition between a two-body attraction, a three-body repulsion, and the kinetic energy plays a crucial role in determining the behaviors of exciton distributions. Numerical simulation of the corresponding nonlinear Schrödinger equation seems to confirm the analysis. Nevertheless, the reason of forming macroscopically ordered exciton states may be more complex than what is expected. Full understanding of

the exciton interactions requires a reliable many-body calculation beyond the mean-field approximation, which is obviously not feasible at the moment. In order to realize the exciton BEC phenomenon, it is in demand to obtain the exciton with even lower combination rate and shorter relaxation time.

Acknowledgments

This work was supported by the National Basic Research Program of China (Grant No. 2005CB32170X),

and National Science Council of Taiwan (Grant No. 96-2112-M-003-008).

-
- ¹ A. K. L.V. Keldysh, Zh. Eksp. Teor. Fiz. **54** (1968).
² L. V. Butov, C. W. Lai, A. L. Ivanov, A. C. Gossard, and D. S. Chemla, Nature **417**, 47 (2002).
³ L. V. Butov, A. C. Gossard, and D. S. Chemla, Nature **418**, 751 (2002).
⁴ C. W. Lai, J. Zoch, A. C. Gossard, and D. S. Chemla, Science **303**, 503 (2004).
⁵ L. V. Butov, L. S. Levitov, A. V. Mintsev, B. D. Simons, A. C. Gossard, and D. S. Chemla, Phys. Rev. Lett. **92**, 117404 (2004).
⁶ L. S. Levitov, B. D. Simons, and L. V. Butov, cond-mat/0403377.
⁷ V. I. Sugakov, cond-mat/0407398.
⁸ V. I. Sugakov, Phys. Rev. B **76**, 115303 (2007).
⁹ A. T. Hammack, M. Griswold, L. V. Butov, L. E. Smallwood, A. L. Ivanov, and A. C. Gossard, Phys. Rev. Lett. **96**, 227402 (2006).
¹⁰ A. High, A. Hammack, L. Butov, L. Mouchliadis, A. Ivanov, M. Hanson, and A. Gossard, cond-mat/0804.4886.
¹¹ S. Yang, A. V. Mintsev, A. T. Hammack, L. V. Butov, and A. C. Gossard, Phys. Rev. B **75**, 033311 (2007).
¹² C. Schindler and R. Zimmermann, Phys. Rev. B **78**, 045313 (2008).
¹³ S. Yang, A. T. Hammack, M. M. Fogler, L. V. Butov, and A. C. Gossard, Phys. Rev. Lett. **97**, 187402 (2006).
¹⁴ M. M. Fogler, S. Yang, A. T. Hammack, L. V. Butov, and A. C. Gossard, Phys. Rev. B **78**, 035411 (2008).
¹⁵ R. Rapaport, G. Chen, D. Snoke, S. H. Simon, L. Pfeiffer, K. West, Y. Liu, and S. Denev, Phys. Rev. Lett. **92**, 117405 (2004).
¹⁶ L. V. Butov, J. Phys.: Condens. Matter **16**, 1577 (2004).
¹⁷ C. S. Liu, H. G. Luo, and W. C. Wu, J. Phys.: Condens. Matter **18** (2006).
¹⁸ L. S. Levitov, B. D. Simons, and L. V. Butov, Solid state Communications **134**, 51 (2005).
¹⁹ L. V. Butov, A. A. Shashkin, V. T. Dolgoplov, K. L. Campman, and A. C. Gossard, Phys. Rev. B **60**, 8753 (1990).
²⁰ H. Benisty, C. M. Sotomayor-Torrès, and C. Weisbuch, Phys. Rev. B **44**, 10945 (1991).
²¹ C. Piermarocchi, F. Tassone, V. Savona, , A. Quattropani, and P. Schwendimann, Phys. Rev. B **53**, 15834 (1996).
²² L. V. Butov, A. L. Ivanov, A. Imamoglu, P. B. Littlewood, A. A. Shashkin, V. T. Dolgoplov, K. L. Campman, and A. C. Gossard, Phys. Rev. Lett. **86**, 5608 (2001).
²³ A. L. Ivanov, P. B. Littlewood, and H. Haug, Phys. Rev. B **59**, 5032 (1999).
²⁴ D. W. Snoke, Y. Liu, Z. Vörös, L. Pfeiffer, and K. West, Solid State Communications **134**, 37 (2005).
²⁵ M. H. Szymanska and P. B. Littlewood, Phys. Rev. B **67**, 193305 (2003).